materials proceedings

MDPI

Proceeding Paper

Co-Gasification of Waste Tyres and Automotive Paint Sludge: Modelling and Simulation with Aspen Plus †

Ndingalutendo Mulaudzi and Athi-enkosi Mavukwana *

Department of Chemical and Materials Engineering, College of Science, Engineering and Technology, University of South Africa (UNISA), c/o Christiaan de Wet & Pioneer Avenue, Florida Campus, Johannesburg 1709, South Africa; 45640424@mylife.unisa.ac.za

* Correspondence: mavukae@unisa.ac.za

† Presented at the 4th International Conference on Applied Research and Engineering, Pretoria, South Africa, 21–23 November 2025.

Abstract

Waste tyres, with their high carbon content and heating value that is greater than that of coal and biomass, present a potential feedstock for energy recovery. Similarly, automotive paint sludge (APS) is a hazardous waste rich in volatile and inorganics compounds, making it difficult to dispose of safely, but it also has potential for thermochemical conversion. Gasification is a thermochemical process which can turn such wastes into syngas, a mixture mainly composed of carbon monoxide and hydrogen that can be utilized to generate power and produce liquid fuels. To deal with challenges of single feedstock gasification, co-gasification combines two or more feedstocks, taking advantage of synergistic interactions to enhance syngas yield and overall efficiency. In this work, Aspen Plus simulation software is used to develop a model for the co-gasification of waste tyres and automotive paint sludge. Sensitivity analysis was performed with the aim of investigating and optimizing the overall process conditions of waste tyre and APS co-gasification. This study investigated the effect of air (*ER*) and water feed (*SFR*) and blend ratios on the adiabatic reaction temperature, product gas composition and heat value of the product syngas. Optimal operating ranges were identified as *ER* = 0.35–0.40 and *SFR* = 1.0–1.2 for tyre gasification, *ER* ≈ 0.50–0.55 for APS-only gasification, and *ER* = 0.40–0.48 with *SFR* = 0.8–1.0 for co-gasification blends. Adiabatic temperatures under recommended conditions were typically 700–800 °C. The LHV of syngas decreased with increasing *ER*, *SFR*, and APS fraction, falling from ~13 MJ/kg for tyre gasification to below 10 MJ/kg for APS-rich cases due to oxidation and dilution by CO_2 and ash. No positive synergistic effect in syngas quality was observed under thermodynamic equilibrium conditions. APS primarily acted as an ash-rich, low-carbon diluent, reducing CO concentration, heating value and adiabatic temperature. However, potential catalytic interactions from APS mineral matter, which are not represented in the equilibrium model, may produce synergistic effects in practical gasifiers.

Keywords: waste tyres; automotive paint sludge; co-gasification; Aspen Plus

Check for updates

Academic Editor: Velaphi Msomi

Published: 7 April 2026

Copyright: © 2026 by the authors. Licensee MDPI, Basel, Switzerland. This article is an open access article distributed under the terms and conditions of the Creative Commons Attribution (CC BY) license.

1. Introduction

The automotive industry, like most industries, is being pushed by environmental concerns and stricter regulations to reduce waste, recycle more, and minimize landfill disposal [1]. The growing demand for vehicles in regions like European Union, the United States, Asia, and Southern Africa is expected to drive a global increase in automobile production, leading to increased generation of waste tyres and automotive paint sludge [2].

According to Yeganeh and Khatamgooya et al., 2023 [3], the painting of vehicles produces an average of 2.5 to 5.0 kg of paint sludge per vehicle. APS is a complex, non-biodegradable waste material consisting of heavy metals, pigments, volatile organic compounds (VOCs) and numerous other toxic substances. APS must be disposed of safely because improper handling can have serious negative effects on the environment. Conventional management methods, such as dewatering followed by landfilling or incineration, are widely used but contribute to climate change and adversely affect ecosystems, air quality, and groundwater and may lead to loss of land for forests or human use [3–5]. According to the waste management hierarchy, recycling, recovery, and reuse should be prioritized over simple disposal [3]. Each year, around 17 million tons of waste tyres is generated globally, yet only 10% is recycled, and as much as 75% is sent to the landfill for bulk storage [6]. Waste tyres can take around 80 to 100 years to decompose naturally, and their bulk storage in landfills requires substantial space [2]. The high carbon and hydrogen contents of waste tyres and automotive paint sludge make them appealing feedstocks for thermochemical energy recovery methods, particularly gasification [5,7].

Gasification is a widely used thermochemical process that produces syngas through the partial oxidation of carbonaceous materials such as coal, biomass, and various other waste streams in an oxygen-limited environment under high temperatures [8,9]. This produces more valuable goods with a broader range of applications than the original feedstock. Gasification achieves high volume reduction, reduced costs and better treatment efficiency, thus attracting a lot of attention over other solid waste treatment technologies [9]. However, single feedstock gasification generally possesses some drawbacks. For example, the gasification of plastics encounters difficulties with feeding and the formation of contaminants; municipal solid waste presents difficulties due to its large volume and high moisture content, whereas biomass is susceptible to seasonal availability [10]. The drawbacks of waste tyre gasification include low tyre char reactivity, loss of catalyst activity and carbon emissions [11,12]. This is mostly because tyres undergo vulcanization during production, which improves their chemical stability and heat resistance. Combined with their high carbon and ash content, this makes tyres challenging to decompose [11–15]. Aside from its high moisture content, APS also contains heavy metals, organic resins, inorganic pigments, organic solvents, and additives, presenting challenges during thermal treatment. Challenges include the decreased syngas heating value, higher tar formation, lower reaction temperatures, and the production of problematic ash or slag, which can result in reactor fouling, slagging, and catalyst poisoning because of the heavy metal content [16–20].

Co-gasification, which involves gasifying a mixture of different wastes at varying ratios, has garnered a lot of attention as a solution to these problems. For instance, when biomass and low-grade coal are co-gasified, the volatile components of the biomass break down quickly, releasing free radicals that react with the coal's organic matter to increase the conversion rate overall. Plus, the hydrogen generated from biomass can quickly interact with free radicals created from coal, preventing their recombination into less reactive secondary tar molecules. Therefore, fuel gases that are high in hydrogen are produced [21].

Air is the most widely used gasifying agent because of its low cost and availability. But the high nitrogen content in air dilutes the product gas, resulting in syngas with a low calorific value. For this reason, steam and oxygen are commonly employed to improve syngas quality [22,23]. Oxygen increases the temperature inside the gasifier by promoting exothermic oxidation reactions, which release heat. The higher temperature improves the conversion of char and volatile matter to gases such as CO and H_2, boosting the calorific value and combustible gas concentration of syngas [24]. Steam gasification promotes endothermic reactions with hydrocarbons, enhancing hydrogen yield and raising the H_2/CO ratio, which improves syngas quality and thermal efficiency. When steam is used

as a co-agent, it not only raises the H_2/CO ratio but also lowers the average temperature in the gasifier, providing process stabilization and reducing the risk of ash melting [25]. Hence, a sensitivity analysis is essential to determine the optimal balance of steam and oxygen that yields syngas with a hydrogen-to-carbon monoxide ratio greater than 1, suitable for fuel and other chemicals such as methanol [26].

This work aims to develop a simplified Aspen Plus (V12.1) flowsheet for the co-gasification of waste tyres and automotive paint sludge (APS) into syngas. The effects of key operating parameters will be examined through sensitivity analysis to determine optimal operating conditions [26].

2. Methodology

The gasification models illustrated in Figures 1–3 were developed using Aspen Plus. The process consists of four main stages: feedstock decomposition (RYield), gasification (RGibbs), gas–solid separation (Cyclone), and syngas cleaning (Separator). The objective of the modelling was to investigate the effects of air supply, expressed as equivalence ratio (*ER*), and the steam-to-fuel ratio (*SFR*) on syngas composition, the H_2/CO ratio and the adiabatic gasification temperature. The equivalence ratio (*ER*) was calculated on a molar oxygen basis as follows [27]:

$$ER = \frac{Actual\ O_2\ supplied}{Stoichiometric\ O_2\ required\ for\ complete\ combustion}$$

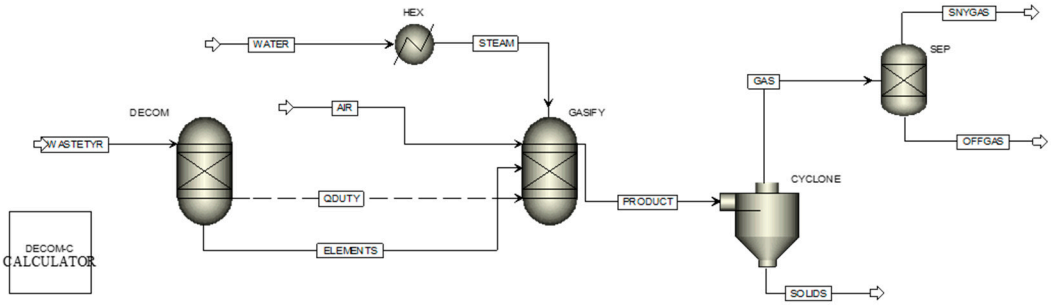


Figure 1. Waste tyre gasification flowsheet.

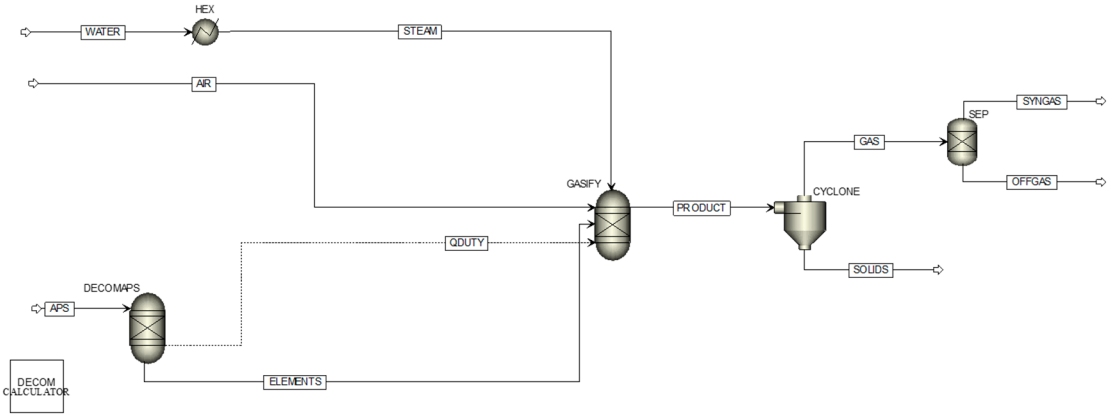


Figure 2. APS gasification flowsheet.

The stoichiometric oxygen demand was calculated from the ultimate analysis of the feedstocks (Table 1), assuming complete conversion of C ⇒ CO_2, H ⇒ H_2O, and S ⇒ SO_2. The nitrogen (N) present in the feedstocks was treated as inert in the stoichiometric oxygen demand calculation and hence was not considered to consume oxygen. Air supplied to the

gasifier was assumed to consist of 21% O_2 and 79% N_2 on a molar basis. The steam-to-fuel ratio (*SFR*) was calculated on a mass basis [28]:

$$SFR = \frac{Mass\ flow\ of\ steam\ supplied}{Mass\ flow\ of\ feedstock\ entering\ the\ gasifier}$$

Sensitivity analysis was carried out by varying *ER* while keeping *SFR* constant, and vice versa.

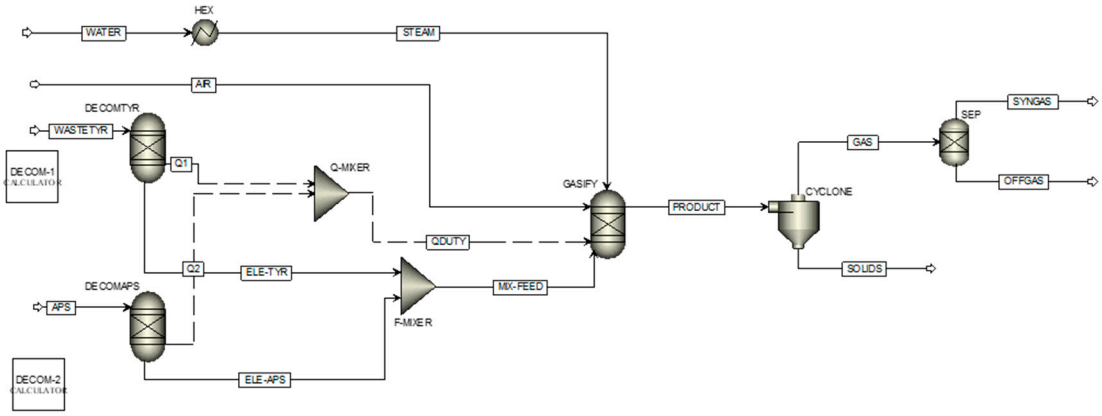


Figure 3. Waste tyre and automotive paint sludge gasification flowsheet.

The Soave–Redlich–Kwong (SRK) equation of state was the property method selected for conventional components for the simulation due to its effectiveness in handling non-polar and weakly polar substances, such as hydrocarbons and light gases (CO_2 and H_2), across a wide range of operating conditions [29]. Waste tyres and automotive paint sludge were defined as non-conventional components, and the HCOALGEN and DCOALIGT models were selected to estimate enthalpy and density using proximate and ultimate analysis. The proximate and ultimate analyses of the feedstocks were taken from [30,31], and the results are shown in Table 1.

Table 1. Results of ultimate and proximate analyses of waste tyres [30] and automotive paint sludge [31].

Feedstock		Waste Tyres	APS
Ultimate analysis (wt.% db)			
	C	79.16	37.55
	H	7.34	6.26
	N	0.60	0.00
	O [1]	1.11	0.77
	S	2.13	0.00
	Cl	0.00	0.00
Proximate analysis (wt.% db)			
	FC	40.28	7.47
	VM	50.06	37.11
	Ash	9.66	55.42
	LHV (MJ/kg)	37.25	18.58

db: dry basis; FC: fixed carbon; VC: volatile matter; LHV: lower heating value; [1] determined by difference.

Three simulation models were developed:

1. Tyre-only gasification;
2. APS-only gasification;
3. Tyre–APS co-gasification.

For single-feed simulations, 100 kg/h of dry feed entered the RYield block at 250 °C and 1 bar. For co-gasification, tyre:APS mass blend ratios of 90:10, 70:30, 50:50, and 30:70 were investigated. The RYield reactor was used to model the pyrolysis of waste tyres and APS. In each case, the RYield converted the non-conventional feedstocks into conventional elemental constituents (C, H, O, N, and S) based on their ultimate and proximate analysis data through the FORTRAN-based simulation calculator. The RYield blocks function at 500 °C and 1 bar [32].

The decomposed products from the RYield are transferred to the RGibbs (GASIFY block), which simulates the gasification stage. In the co-gasification model, the heat duties from DECOMTYR (Q1) and DECOMAPS (Q2) are first combined in the Q-MIXER block before it is transferred to the GASIFY reactor. The waste tyre-only and APS-only models use a single QDUTY stream. These heat streams provide the required energy to maintain adiabatic operation of the gasifier. The RGibbs reactor operates at 1 bar, with its temperature determined by the gasifying agents and the heat supplied from RYields. The equilibrium compositions of the PRODUCT stream are calculated by minimizing Gibbs free energy. Equilibrium calculations only take into account the gas phase components: H_2, CO, CO_2, CH_4, H_2O, N_2, H_2S, C_2H_2, C_2H_4 and C_2H_6. Since higher hydrocarbons and tars are products of non-equilibrium reactions, they are not taken into consideration [26,33,34].

This modelling approach is based on thermodynamic equilibrium assumptions, which consider that the reaction time is sufficiently long for all reactions to reach equilibrium and that the reactor contents are perfectly mixed under uniform temperature and pressure conditions. Tar formation is a kinetically controlled non-equilibrium reaction associated with incomplete cracking of volatiles during pyrolysis and cannot be accurately represented in a Gibbs free energy minimization reactor. Therefore, the exclusion of tar and heavy hydrocarbons allows the model to estimate the maximum theoretical syngas potential and to analyze the parametric effects of *ER* and *SFR*. It is acknowledged that in a real gasifier, tar formation would decrease H_2 and CO concentrations, lower the LHV of the product gas, and necessitate gas cleaning steps [26,33–35].

Gasifying agents consist of air and steam. Before being fed into the RGibbs (GASIFY) block, water is preheated at 1 bar to 110 °C to generate steam, while air (79% N_2, 21% O_2) is fed at 25 °C and 1 bar. The reactor accounts for partial oxidation, reduction, steam reforming, and water–gas shift reactions. The simulations were completed at atmospheric pressure for simplicity in initial design and to match common conditions in the literature. However, higher pressures may affect syngas composition by increasing CH_4 content, slightly reducing H_2, and affecting tar formation and heat transfer [35,36]. This can be explained by the inhibitory effect of high pressure on pyrolysis and volatile release, which increases char yield but reduces its reactivity, lowering CO and H_2 formation rates [37]. Pressurized operation also allows for the production of compressed syngas that can be directly used in synthesis reactions and may also enhance the overall process efficiency through heat recovery. However, it may reduce cold gas efficiency because of increased methane formation and heat losses associated with compression [36,38], and pressure-resistant equipment is required, including reinforced gasifiers and compressors, which increases capital and operational costs.

The PRODUCT stream from the GASIFY block enters a cyclone separator. The cyclone separates unreacted char and ash (SOLIDS stream) from the raw gas (GAS stream). After that, the GAS stream is fed to a separation (SEP) block, which simulates gas cleaning, assuming complete removal of impurities. The final cleaned syngas contains only H_2, CO, CH_4, CO_2, C_2H_2, C_2H_4 and C_2H_6. Co-gasification of APS raises environmental concerns because of toxic compounds and heavy metals in the feedstock. While the simulation assumes complete removal of impurities in the SEP block, a real operation would

need filtration, scrubbers, or catalytic cleaning of the raw syngas to meet environmental regulations and ensure safe use. In addition, careful handling and disposal of the resulting ash is necessary to prevent contamination to the environment [37,39]. The simulation assumptions were:

1. Gasification/co-gasification operates under steady state conditions.
2. Ash is inert and does not participate in reactions.
3. All the sulphur in the feedstock is transformed H_2S.
4. Char is 100% carbon. Tars and higher hydrocarbons are neglected because of the equilibrium model assumption [26,33,34].

The assumption that ash is inert represents a simplification of the real gasification process. In practical systems, the high ash content in APS can affect the reactor performance. Elevated ash levels may promote slagging and agglomeration, which can affect heat transfer and reactor operability at high temperatures [40]. In addition, the mineral species commonly present in the ash, such as alkali and alkaline earth metals (K and Ca) and iron oxides, can exhibit catalytic behaviour, enhancing reactions such as tar cracking and the water–gas shift reaction, thereby altering syngas composition and the H_2/CO ratio. Conversely, volatilization of alkali species at high temperatures may contribute to ash deposition and fouling. These physicochemical effects have not been included by the present equilibrium models and represent a limitation when translating the results to industrial-scale systems [41].

To evaluate the predictive reliability of the Aspen Plus equilibrium model, the tyre simulation results were compared with experimental data from the study by Serrano et al., 2022 [42], under similar *ER* and *SFR* conditions. Serrano et al., 2022 [42], investigated gasification of waste tyres in a fluidized bed reactor. The model captures the major gasification trends with *ER*, although deviations in absolute values are observed. Hydrogen and CO are overestimated by the model, while CH_4 and light hydrocarbons are strongly underpredicted. Comparison can be seen in Table 2. These differences arise from the thermodynamic equilibrium assumption in the RGibbs reactor, which promotes complete steam reforming, water–gas shift, and char gasification reactions while neglecting kinetic limitations, tar formation and incomplete reforming that occur in real fluidized bed gasifiers. The CO_2 content is correspondingly lower in the model because equilibrium conditions favour carbon conversion through the Boudouard and steam–carbon reactions toward CO, while real reactors retain more CO_2 due to kinetic and mass transfer limitations. The model also underpredicts temperature compared with experimental data but reproduces the increasing temperature trend with *ER*. Despite quantitative differences, the directional agreement of H_2 decrease, CO increase and temperature rise with *ER* demonstrates that the model reliably represents process behaviour and is suitable for parametric and sensitivity analysis, with predicted compositions representing ideal equilibrium limits rather than exact reactor outputs.

Due to the limited availability of experimental gasification data for APS, model comparison was conducted using sewage sludge gasification experiments reported by Gil-Lalaguna et al., 2014 [43], and Schweitzer et al., 2018 [44] (Table 3). Sewage sludge and APS exhibit comparable thermochemical characteristics, including high ash content and lower fixed carbon compared to tyres. Experimental gas compositions from Gil-Lalaguna et al., 2014 [43], were converted to an N_2- and H_2S-free basis to ensure consistency with the simulation output. Reported lumped C_2 hydrocarbons (C_2Hx) were compared with the sum of C_2H_2, C_2H_4, and C_2H_6 predicted by the model. Although quantitative differences exist, the model reproduces the key gasification trends observed experimentally. Both the models and experiments show that increasing oxidizing severity leads to lower CO and CH_4 concentrations because of enhanced improved oxidation and steam-reforming

reactions, while CO_2 becomes more dominant. Hydrogen is a main product in both cases, reflecting the contribution of steam reforming and water–gas shift reactions. It is worth noting that the Aspen Plus model assumes thermodynamic equilibrium under ideal conditions, unlike real reactors that deal with kinetic limits, heat losses, incomplete tar cracking and even catalytic boosts from ash minerals. That is why the model shows higher H_2 and CH_4 contents but a lower CO content than the experiments: it captures the theoretical max syngas potential, not real-world constraints. In practical reactors, the char–gas reactions and mass transfer limitations maintain higher CO concentrations than those predicted under equilibrium. The absence of C_2 hydrocarbons in the model further reflects the equilibrium assumption, which favours complete cracking of heavier hydrocarbons. The simulated model temperature values are adiabatic equilibrium, whereas the experimental temperatures are externally controlled. The lower predicted temperatures arise from the high ash fraction of APS lowering the net heat release during oxidation. In real gasifiers, heat transfer from bed material and external heating sustain higher temperatures [45]. The contrasting CO_2 behaviour between tyre and APS comparisons reflects their different H/C and O/C ratios and ash contents, which alter the equilibrium distribution of carbon between CO and CO_2.

Table 2. Comparison of tyre-only gasification model with Serrano et al., 2022 [42].

Parameter	Serrano et al., 2022 [42]			Tyre Model		
ER	0.13	0.20	0.27	0.13	0.20	0.27
SFR	0.39	0.39	0.39	0.39	0.39	0.39
H_2 (vol%)	27.8	28.7	23.3	58.7	52.9	47.4
CO (vol%)	14.3	15.5	16.4	20.3	32.6	42.3
CH_4 (vol%)	15.7	12.2	9.8	6.0	2.6	1.3
CO_2 (vol%)	26.5	33.3	40.6	15.0	11.9	8.9
C_2H_2 (vol%)	0.3	0.1	0.1	2.6×10^{-11}	1.1×10^{-10}	2.7×10^{-10}
C_2H_4 (vol%)	7.5	4.4	0.3	6.1×10^{-8}	6.2×10^{-8}	5.7×10^{-8}
C_2H_6 (vol%)	0.4	0.3	0.2	4.0×10^{-7}	1.4×10^{-7}	5.6×10^{-8}
Temp (°C)	847.1	855.6	860.2	621.6	669.5	705.3
LHV (MJ/Nm^3)	11.98	7.79	6.39	10.99	10.66	17.50

Table 3. Comparison of APS-only gasification model with Gil-Lalaguna et al., 2014 [43], and Schweitzer et al., 2018 [44].

Parameter	Gil-Lalaguna et al., 2014 [43]	APS Model	Schweitzer et al., 2018 [44]	APS Model
ER	0.32	0.32	-	0.35
SFR	0.39	0.39	1	1
H_2 (vol%)	29.1	46.4	46.8	44.8
CO (vol%)	18.7	6.9	9.3	3.4
CH_4 (vol%)	5.4	14.2	13.9	14.9
CO_2 (vol%)	44.7	32.5	26.4	36.9
C_2H_x (vol%)	2.9	7.03×10^{-7}	3.5	
Temp (°C)	810	508 [1]	760	475 [1]
LHV (MJ/kg)	-	13	17	12

[1] Model temperatures are adiabatic equilibrium values.

3. Results and Discussion

The influence of the equivalence ratio (*ER*) and steam-to-fuel ratio (*SFR*) on the syngas composition and adiabatic gasification temperature was investigated in this work. The impact of ER on syngas composition and adiabatic temperature at a fixed *SFR* of 0.8 is

shown in Figure 3 for waste tyre gasification, APS gasification and tyre–APS co-gasification at blend ratios (tyre:APS) of 90:10, 70:30, 50:50 and 30:70. *ER* and *SFR* are major operating parameters that affect the gasification performance. The ER determines the amount of oxygen available for partial oxidation, affecting reactor temperature, syngas composition, and thermal efficiency. The *SFR* controls the amount of steam supplied, which affects hydrogen yield, methane formation, and the H_2/CO ratio [13]. A list of possible reactions taking place during gasification are listed in Table 4 for reference during discussions.

Table 4. Gasification reactions [33].

Reactants				Products	Rxn Number
C	+	O_2	→	CO_2	R1
C	+	CO_2	↔	2CO	R2
C	+	0.5 O_2	↔	CO	R3
C	+	2 H_2	↔	CH_4	R4
C	+	H_2O	↔	CO + H_2	R5
CO	+	H_2O	↔	CO_2 + H_2	R6
CH_4	+	H_2O	↔	CO + 3H_2	R7
H_2	+	S	→	H_2S	R8
0.5 N_2	+	1.5 H_2	↔	NH_3	R9

For waste tyre gasification (Figure 4a), hydrogen is the primary syngas component between *ER* values of 0.18 and 0.40, peaking at a 0.54 mole fraction at *ER* = 0.18. As the ER increases beyond this point, hydrogen decreases while CO rises from an *ER* of 0.44 to 0.57, reaching a maximum molar fraction of 0.44 before declining. CH_4 and C_2 hydrocarbons decrease rapidly with the *ER*, disappearing completely above *ER* = 0.8 due to being consumed in the oxidation and reforming reactions (R4, R6 and R7). CO_2 keeps climbing as the *ER* increases, showing the increasing dominance of reaction R1. Serrano et al., 2022 [42], observed similar trends in their experiments on waste tyre gasification in a bubbling fluidized bed. The same trends were also reported by Li et al. in 2024 [33] using Aspen Plus models. The adiabatic temperature increases sharply with the *ER*, reaching nearly 1900 °C at *ER* = 1.0 due to the increasing available oxygen contributing to complete combustion. These temperatures are higher than what is practical for real-world gasifiers despite the fact that this trend is thermodynamically consistent due to greater exothermic oxidation processes. Most gasification processes run at relatively high gasification temperatures, typically between 1100 and 1300 °C, mainly to minimize tar formation, though fluidized bed gasifiers are an exception, functioning at lower temperatures of around 800 to 850 °C [46]. At excessively high temperatures, severe operational issues such as slagging, fouling, bed agglomeration (in fluidized beds), and refractory material degradation may occur [47]. Additionally, high *ER* operation needs higher air supply, reducing cold gas efficiency and shifting the process towards combustion rather than gasification [47].

For APS-only gasification (Figure 4b), similar directional trends are observed, but with marked compositional differences. APS produces lower temperatures across the *ER* range due to its high ash fraction and lower fixed carbon content, which dilute the reactive portion of the fuel. Hydrogen production is enhanced relative to tyre gasification at moderate *ER* values between approximately 0.24 and 0.48, where H_2 increases sharply and reaches a maximum at *ER* = 0.48. This behaviour reflects stronger steam participation and the water–gas shift reaction (R6), while the CO content remains lower due to the limited fixed carbon availability in APS. CO_2 becomes the dominant carbon species at a high *ER*, indicating oxidation of the small fixed carbon fraction. Methane is rapidly consumed, and C_2 hydrocarbons remain negligible, consistent with equilibrium cracking at elevated temperatures.

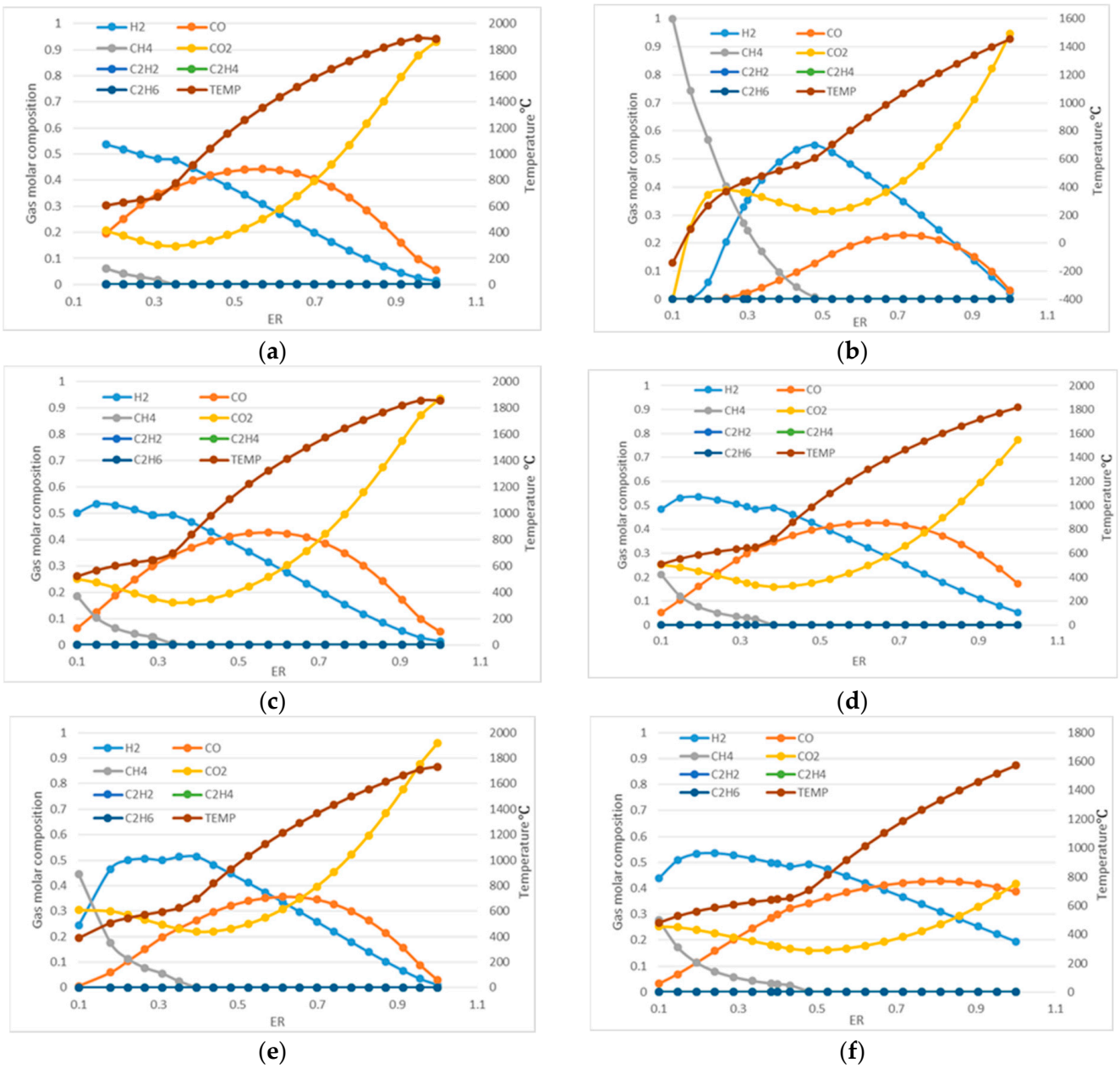


Figure 4. Effect of *ER* on product gas and adiabatic temperature: (**a**) waste-tyre-only gasification; (**b**) APS-only gasification; (**c**) co-gasification with 90:10 ratio of waste tyre to APS; (**d**) co-gasification with 70:30 ratio of waste tyre to APS; (**e**) co-gasification with 50:50 ratio of waste tyre to APS; (**f**) co-gasification with 30:70 ratio of waste tyre to APS.

For co-gasification, the *ER* response progressively shifts from tyre-dominated to APS-dominated behaviour as the APS fraction increases (Figure 4c–f). The 90:10 blend behaves similarly to tyre-only gasification but shows slightly lower temperature and CO production. When the APS content is increased to ratios of 70:30 and 50:50, there is a reduction in reactor temperature and CO concentration while there is a moderate increase in H_2 and CO_2 fractions. At the highest APS content (30:70 blend), the gas composition is more oxidized, with lower CO and higher CO_2 contents and a decreased temperature profile. For all blends, the methane concentration declines with the *ER* and becomes negligible at a high *ER*, indicating dominance of reforming reactions. Overall, these results indicate that blending APS with tyres mainly produces a dilution effect rather than a synergistic enhancement. The addition of APS lowers the reactor temperature, suppresses CO formation, and shifts carbon toward CO_2 through equilibrium oxidation and water–gas shift reactions. These

results confirm the classic trade-off in gasification: a low *ER* favours high H_2 yield but insufficient temperature, while higher a *ER* improves temperature but dilutes syngas with CO_2 [48]. *ER* values above ~0.6 therefore represent thermodynamic limits rather than practical operating conditions, especially for ash-rich APS blends where slagging risks are significant.

For *SFR* sensitivity analysis, the *ER* was fixed at a representative gasification value for each feedstock and blend, selected based on the *ER* range that produced stable gasification temperatures and meaningful syngas composition in the *ER* sensitivity study. Because APS contains higher ash and lower fixed carbon contents than tyres, a slightly higher *ER* was required to maintain adequate reactor temperature. Figure 5 shows the effects of *SFR* on gas molar composition and adiabatic temperature for tyre-only gasification (*ER* = 0.35), APS-only gasification (*ER* = 0.50), and the different tyre–APS blends (*ER* = *0.35* for 90:10 and 70:30, *ER* = 0.40 for 50:50, and *ER* = 0.45 for 30:70). Across all cases, increasing the *SFR* leads to a clear rise in hydrogen concentration, while the concentrations of CO and light hydrocarbons decline. This behaviour is expected because of the water–gas reaction (R5) and steam reforming (R7); however, in R6, the CO shift reaction consumes more CO than generated in R5 and R7. Hence, as the *SFR* increases, H_2 and CO_2 contents increase while the CO content decreases. The rise in the *SFR* favours the steam reforming reaction, thus converting hydrocarbons into H_2 and CO_2. In APS-only gasification, the increase in hydrogen with the *SFR* is more moderate than for tyres because APS contains a lower fixed carbon content and fewer reformable hydrocarbons. As a result, there is less reactive carbon available for the char–steam, steam reforming and water–gas shift reactions that generate H_2. However, CO declines sharply with *SFR*, and CO_2 becomes the dominant carbon species, indicating stronger oxidation and shift conversion relative to carbon gasification. For co-gasification blends, the response to *SFR* lies between the two single-feed cases. Blends with higher tyre fractions (90:10 and 70:30) show stronger H_2 improvement with the *SFR* due to greater volatile and hydrocarbon reforming potential. As the APS fraction increases (50:50 and 30:70), the incremental H_2 gain with the *SFR* becomes smaller, while CO_2 increases more noticeably, reflecting the ash-rich, low-carbon nature of APS diluting the reactive fuel fraction.

The adiabatic gasification temperature decreases with an increasing *SFR* in all cases. Steam acts as a thermal moderator because its high specific heat absorbs part of the reaction heat, and steam reforming reactions (R5 and R7) are endothermic [26,36]. Therefore, higher *SFR* values reduce the net reactor temperature despite enhancing hydrogen production.

Figure 6 displays the impact of the *ER* and *SFR* on the H_2/CO ratio. In all plots, the H_2/CO ratio increases as the *ER* declines and the *SFR* rises. For tyre-only gasification, the H_2/CO ratio responds strongly to the *SFR*, and in contrast, APS-only gasification shows a more moderate increase in the H_2/CO ratio with the *SFR* due to the compositional effects discussed earlier, particularly the higher fixed carbon and volatile compound contents of tyres versus the ash-rich nature of APS. The co-gasification blends exhibit intermediate behaviour, with higher APS fractions generally yielding higher H_2/CO ratios at the same *ER* due to enhanced CO_2 formation and reduced CO production. An H_2/CO molar ratio close to 2, which is desirable for Fischer–Tropsch synthesis, is achievable mainly at low *ER* and high *SFR* conditions. However, these operating points correspond to relatively low adiabatic temperatures (typically below ~650 °C in the equilibrium model), which are insufficient for stable, tar-minimized gasification in practical systems. Thus, although thermodynamically favourable for syngas upgrading, such conditions represent theoretical limits rather than directly viable industrial operating regimes.

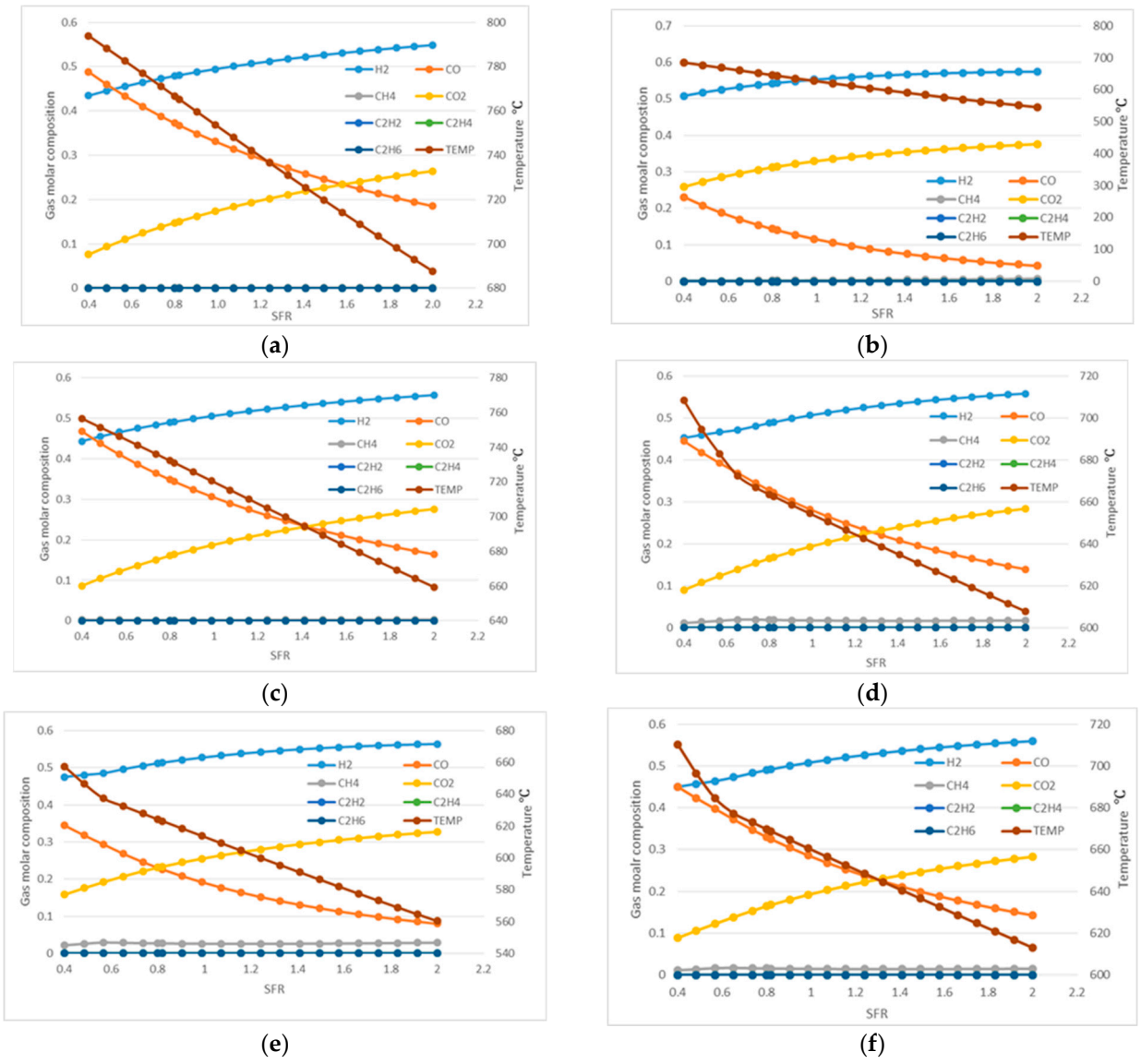


Figure 5. Effect of *SFR* on product gas and adiabatic temperature: (**a**) waste-tyre-only gasification; (**b**) APS-only gasification; (**c**) co-gasification with 90:10 ratio of waste tyre to APS; (**d**) co-gasification with 70:30 ratio of waste tyre to APS; (**e**) co-gasification with 50:50 ratio of waste tyre to APS; (**f**) co-gasification with 30:70 ratio of waste tyre to APS.

Figure 7 shows the influence of the blending ratio between waste tyres and APS on syngas composition at fixed operating conditions, *ER* = 0.4 and *SFR* = 0.8. Increasing the APS fraction leads to a clear reduction in the CO concentration and a steady increase in CO_2, while H_2 shows only moderate variation. The hydrogen concentration increases from tyre-only gasification to a maximum at 50% APS, indicating enhanced contribution of steam gasification and the water–gas shift reaction. However, at higher APS fractions, hydrogen stabilizes due to dilution of reactive carbon by ash. CO_2 decreases continuously with APS addition, reflecting a lower fixed carbon content and stronger shift conversion toward CO_2. Methane remains negligible at low APS fractions but rises sharply in APS-rich blends, consistent with lower adiabatic temperatures and equilibrium favouring methanation. Increasing APS shifts the syngas from a CO-rich tyre-derived gas toward a more oxidized, methane-containing gas typical of ash-rich sludge-type feedstocks.

https://doi.org/10.3390/materproc2026031002

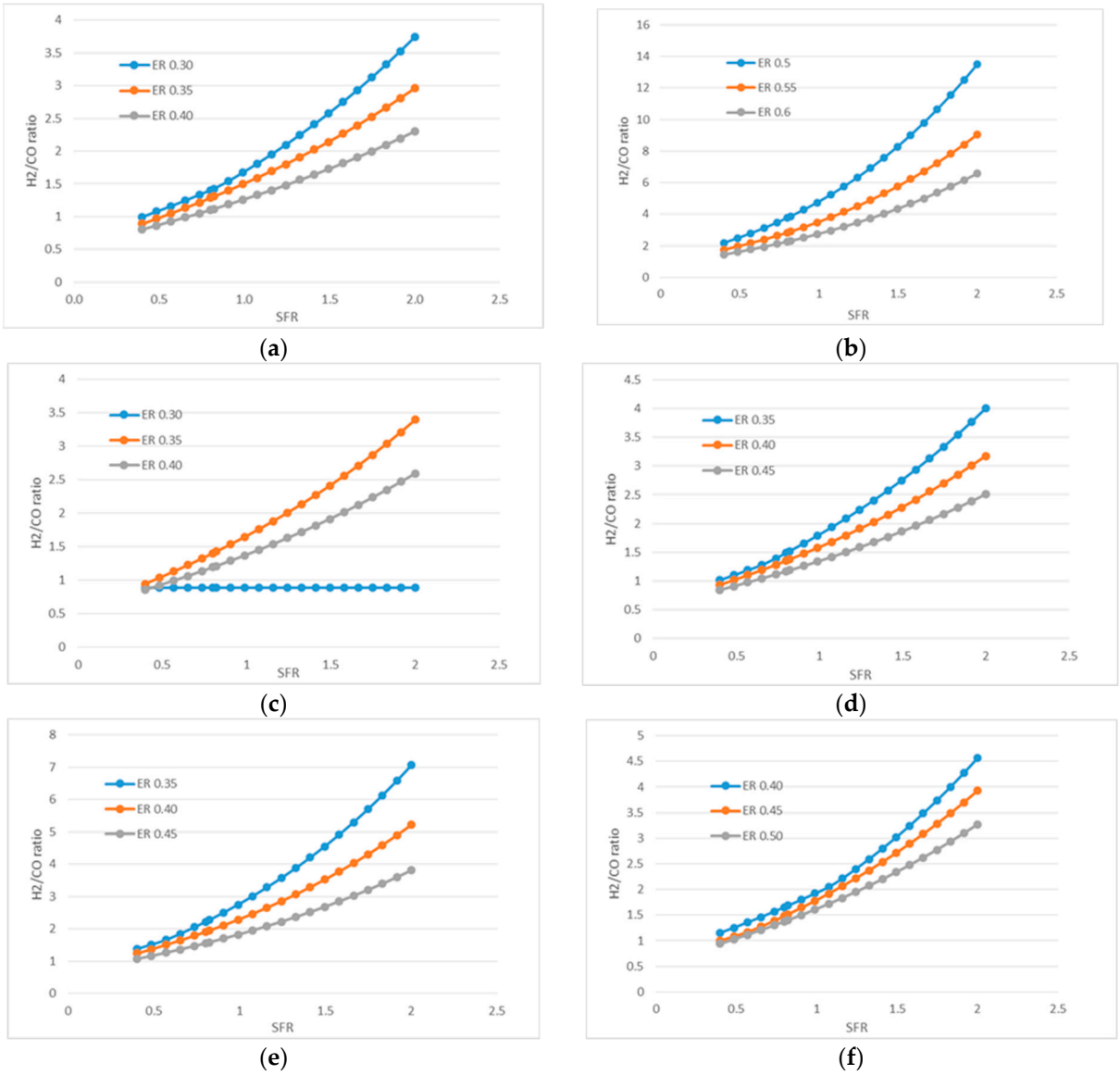


Figure 6. Effect of *ER* and *SFR* on H_2/CO ratio: (**a**) waste-tyre-only gasification; (**b**) APS-only gasification; (**c**) co-gasification with 90:10 ratio of waste tyre to APS; (**d**) co-gasification with 70:30 ratio of waste tyre to APS; (**e**) co-gasification with 50:50 ratio of waste tyre to APS; (**f**) co-gasification with 30:70 ratio of waste tyre to APS.

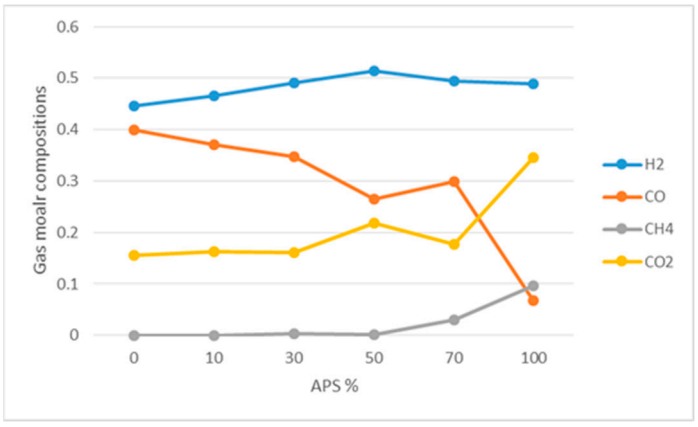


Figure 7. Effects of different ratios of tyre and APS on gas molar composition.

The recommended operating conditions and their gas molar compositions obtained from the models are presented Table 5. As the APS fraction increases, higher *ER* values are required to compensate for its higher ash content and lower fixed carbon content, which dilute the reactive fuel portion and reduce heat release. Consequently, the optimal *ER* gradually increases from tyre-only to APS-only gasification. The lower heating value (LHV) of the product syngas decreases with increasing *ER* and *SFR* and with increasing APS fraction in the feed blend. A higher *ER* promotes greater oxidation of combustible gases (CO, H_2, and CH_4) into CO_2, while a higher *SFR* enhances steam reforming and the water–gas shift reaction, which reduce CO and hydrocarbon contents. In addition, APS contains a higher ash fraction and lower fixed carbon content than tyres, resulting in greater dilution of combustible species and a lower energy density of the product gas. These combined effects explain the gradual reduction in LHV observed across the recommended operating conditions as the blend shifts from tyre-only to APS-rich gasification.

Table 5. Recommended operating conditions.

Tyre:APS	ER	SFR	TEMP	H_2	CO	CH_4	CO_2	LHV	H_2/CO
			°C		Gas molar fraction			MJ/kg	
100:0	0.35	1.20	747	0.51	0.29	7.5×10^{-4}	0.15	12.13	1.73
90:10	0.35	1.00	721	0.51	0.31	2.0×10^{-3}	0.17	12.45	1.73
70:30	0.40	1.00	755	0.50	0.32	7.0×10^{-4}	0.20	12.30	1.58
50:50	0.40	0.80	700	0.51	0.26	2.2×10^{-3}	0.24	12.13	1.94
30:70	0.48	1.00	795	0.49	0.32	0.00	0.25	12.10	1.51
0:100	0.55	0.60	784	0.48	0.22	4.1×10^{-5}	0.26	9.63	1.96

The LHV of the product syngas was calculated using the mole fractions of the main combustible components in the syngas as follows:

$$LHV(MJ/Nm^3) = \frac{(123.36 * \%CO + 107.98 * \%H_2 + 358.18 * \%CH_4)}{1000}$$

where $\%CO$, $\%H_2$ and $\%CH_4$ are the mole percentages of CO, H_2 and CH_4 in the syngas, respectively. By dividing the volumetric LHV by the gas mixture density, the LHV in MJ/kg was determined. Water vapour and non-combustible gases (CO_2 and N_2) were assumed to have no effect on the LHV, and the gas mixture was considered to be dry [49].

The developed models are based on thermodynamic equilibrium and therefore represent the maximum theoretical gasification performance rather than real reactor behaviour. The equilibrium approach assumes infinite reaction time and perfect mixing and uniform temperature and pressure while neglecting kinetic limitations and transport effects. Consequently, H_2 and CO concentrations may be overestimated, and the generation of CH_4, CO_2 and heavier hydrocarbons may be underestimated compared to practical systems. The lack of consideration of tar formation/composition, which needs reaction kinetics, has also been cited as one of the major reasons for the overestimation of H_2 in the equilibrium models compared to the experimental systems [35,50]. In practical gasifiers, incomplete char conversion and tar formation would reduce syngas yield, usable quality, and foul equipment and require gas cleaning [50] compared to equilibrium predictions. However, the direction of the reported trends with the *ER* and *SFR* remains reliable, since changes in oxidizing and steam conditions mainly shift thermodynamic equilibria [51], which are well captured by the models. The assumption of ideal gas behaviour introduces minimal error under high-temperature and low-pressure conditions. Numerical uncertainties related to thermodynamic property data and solver convergence may influence absolute values but are not expected to alter the observed parametric trends. Therefore, the model is most

suitable for comparative and sensitivity analyses rather than exact performance prediction. The equilibrium model does not capture the catalytic role of minerals found in APS ash. APS has plenty significant amounts of metal oxides like TiO_2, Al_2O_3, CaO, Na_2O and MgO. These metal oxides could catalyze gasification reactions [14], promote cracking of tars, boost the water–gas shift reaction (R6), and speed up char–steam gasification (R5), shifting syngas makeup beyond what thermodynamics alone predict [5,8,31,51]. Table 6 compares the mineral composition of APS with that of a conventional fluid catalytic cracking (FCC) catalyst, illustrating the presence of catalytically active oxides in APS. Practical gasification experiments would prove to be helpful in quantifying catalytic effects, validating the model predictions and measuring the effects of the chemical composition of the ash.

Table 6. APS mineral composition compared to FCC catalyst.

Element	APS (Khezri et al., 2012) [52]	FCC Catalyst (Le-Phuc et al., 2018) [53]
Al_2O_3	18.01 wt%	45.90 wt%
SiO_2	2.15 wt%	46.46 wt%
TiO_2	54.21 wt%	3.53 wt%
Fe_2O_3	0.43 wt%	1.10 wt%
MgO	0.66 wt%	0.07 wt%
Na_2O	1.30 wt%	0.24 wt%
CaO	2.30 wt%	0.27 wt%

4. Conclusions

Thermodynamic equilibrium models for waste tyre gasification and its co-gasification with automotive paint sludge were built in Aspen Plus to assess how the ER and SFR influence syngas composition and adiabatic temperature. Based on the results, for tyre gasification, optimal performance was obtained at *ER* = 0.35–0.40 and *SFR* = 1.0–1.2, where hydrogen-rich syngas ($H_2 \approx 0.50$ mol fraction) was produced at acceptable adiabatic temperatures (>650 °C). APS-only gasification required a higher *ER* (0.50–0.55) to compensate for its high ash and low fixed carbon contents, resulting in more oxidized syngas with higher CO_2 and lower LHV. In co-gasification, increasing the APS fraction progressively reduced the CO concentration, increased CO_2 formation, and lowered adiabatic temperature due to dilution of reactive carbon and reduced exothermic heat release. The absence of a strong synergistic effect with the blends confirms that APS mostly acts as an inert, ash-rich diluent under equilibrium conditions rather than improving reactivity. Hydrogen yield increased with the *SFR* across all cases due to steam reforming (R5 and R7) and the water–gas shift reaction (R6), while CO decreased and CO_2 increased [54]. Rising *ER* improved oxidation reactions (R1 and R3), increased temperature and shifted syngas toward more oxidized compositions. The H_2/CO ratio increased at a lower *ER* and a higher *SFR*, but the conditions that produced $H_2/CO \approx 2$ were associated with lower temperatures that may not be industrially practical without additional heat input.

The LHV of produced gas decreased with increasing *ER*, *SFR*, and APS fraction, falling from ~13 MJ/kg for tyre gasification to below 10 MJ/kg for APS-rich blends. This decline is attributed to oxidation of combustible species and dilution by CO_2 and inert ash-derived effects [9,14]. Under the recommended conditions, the produced syngas is most suitable for hydrogen production (via water–gas shift and PSA) and for power generation, whereas Fischer–Tropsch synthesis would require further gas conditioning and CO_2 removal. Because the model is based on thermodynamic equilibrium, it represents the maximum theoretical gasification performance. Kinetic limitations, tar formation and catalytic effects of APS mineral matter are not captured. The high TiO_2, Al_2O_3, and alkaline oxides present in APS ash suggest potential catalytic behaviour in real systems,

particularly for tar cracking and water–gas shift enhancement. Therefore, it is recommended to conduct experiments to quantify ash catalytic effects, evaluate slagging behaviour and verify syngas quality under practical reactor conditions. Overall, the developed models provide a reliable tool for comparative and sensitivity analysis of tyre and APS gasification, supporting process optimization and preliminary design while highlighting the importance of feedstock ash chemistry in real gasifier performance.

Author Contributions: Conceptualization, A.-e.M.; methodology, software, validation, formal analysis, investigation, and writing—original draft preparation, N.M.; writing—review and editing, supervision, project administration, and funding acquisition, A.-e.M. All authors have read and agreed to the published version of the manuscript.

Funding: This research and the APC were funded by the National Research Foundation of South Africa (NRF), grant number RA231202197463.

Institutional Review Board Statement: This Non-human research study was reviewed by College of Science, Engineering and Technology_ School of Engineering_ERC on 12/02/2024 in compliance with the Unisa Policy on Research Ethics and the Standard Operating Procedure on Research Ethics Risk Assessment. Ethics Approval from 12/02/2024 to 12/02/2027, ref#:2743.

Informed Consent Statement: Not applicable.

Data Availability Statement: Data will be made available on request to the corresponding author.

Acknowledgments: The authors are grateful for the funding provided by the NRF and University of South Africa.

Conflicts of Interest: The authors declare no conflicts of interest. Equally, the funders had no role in the design of the study; in the collection, analyses, or interpretation of data; in the writing of the manuscript; or in the decision to publish the results.

References

1. Vijaya, A.; Meisterknecht, J.P.S.; Angreani, L.S.; Wicaksino, H. Advancing sustainability in the automotive sector: A critical analysis of environmental, social, and governance (ESG) performance indicators. *Clean. Environ. Syst.* **2025**, *16*, 100248. [CrossRef]
2. Nkosi, N.; Mthombeni, N.H. An inventory analysis of waste tyre generation and management in South Africa. *Waste Manag.* **2025**, *194*, 353–365. [CrossRef] [PubMed]
3. Yeganeh, B.; Khatamgooya, A. The feasibility study of stabilizing the automotive paint sludge by recycling, to produce green concrete blocks, considering environmental and mechanical factors. *J. Mater. Cycles Waste Manag.* **2023**, *25*, 931–943. [CrossRef]
4. Salmani, J.H.; Yousefi, M.; Sanjarifard, A.; Nowee, S.M.; Asgari, A.; Sedaghat, E.; Lakzian, K. An environmental-friendly procedure for recycling automotive paint sludge. *Recent Prog. Sci.* **2025**, *2*, 8. [CrossRef]
5. Ruffino, B.; Campo, G.; Idris, S.S.; Salihoglu, G.; Zanetti, M. Automotive Paint Sludge: A Review of Pretreatments and Recovery Options. *Resource* **2023**, *12*, 45. [CrossRef]
6. Soprych, P.; Czerski, G.; Grzywacz, P. Studies on the Thermochemical Conversion of Waste Tyre Rubber—A Review. *Energies* **2024**, *17*, 14. [CrossRef]
7. Carmo-Calado, L.; Hermoso-Orzaez, M.J.; Mota-Panizio, R.; Guiherme-Garcia, B.; Brito, P. Co-Combustion of Waste Tyres and Plastic-Rubber Wastes with Biomass Technical and Environmental Analysis. *Sustainability* **2020**, *12*, 1036. [CrossRef]
8. Śpiewak, K. Gasification of Sewage Sludge—A Review. *Energies* **2024**, *17*, 4476. [CrossRef]
9. Jiang, W.; Tao, J.; Zhong, X.; Ye, Y.; Kang, J.; Tang, Q.; Liu, D.; Ren, Y.; Li, D.; Cai, H.; et al. Co-gasification of rural solid waste and biomass in rural areas: Simulation and plant-scale process. *Environ. Res.* **2023**, *235*, 116684. [CrossRef]
10. Mishra, R.; Singh, E.; Kumar, A.; Ghosh, A.; Lo, S.; Kumar, S. Co-gasification of solid waste and its impact on final product yields. *J. Clean. Prod.* **2022**, *374*, 133989. [CrossRef]
11. Oboirien, B.O.; North, B.C. A review of waste tyre gasification. *J. Environ. Chem. Eng.* **2017**, *5*, 5169–5178. [CrossRef]
12. Mavukwana, A.; Stacey, N.; Fox, F.A.; Sempuga, B.C. Thermodynamic comparison of pyrolysis and gasification of waste tyres. *J. Environ. Chem. Eng* **2021**, *9*, 105163. [CrossRef]
13. Fajimi, L.I.; Oboirien, B.O.; Adams, T.A., II. Waste tyre gasification Processes: A bibliometric Analysis and comprehensive review. *Fuel* **2024**, *368*, 131684. [CrossRef]

14. Czerski, G.; Spiewak, K.; Makowska, D.; Grycova, B. Study on steam co-gasification of waste tyre char and sewage sludge. *Energies* **2023**, *16*, 2156. [CrossRef]
15. Muzenda, E. A Comparative Review of Waste Tyre Pyrolysis, Gasification and Liquefaction (PGL) Processes. *UJContent*; University of Johannesburg, 2014. Available online: https://ujcontent.uj.ac.za/esploro/outputs/journalArticle/A-comparative-review-of-waste-tyre/9913489507691#file-0 (accessed on 30 March 2026).
16. Yang, R.; Wang, Z.; Cheng, M.; Yang, Y.; Huang, Z.; Cen, Q.; Zhao, Y.; Zhou, T.; Liu, Z.; Li, B. Chemical looping gasification of automotive paint sludge with red mud oxygen carrier for flammable gas production. *Chem. Eng. J.* **2024**, *497*, 154676. [CrossRef]
17. Kirsanovs, V.; Žandeckis, A. Investigation of Biomass Gasification Process with Torrefaction Using Equilibrium Model. *Energy Procedia* **2015**, *72*, 329–336. [CrossRef]
18. Naryanto, R.F.; Enomoto, H.; Cong, A.V.; Fukadu, K.; Zong, Z.; Delimayanti, M.K.; Chunti, C.; Noda, R. The Effect of Moisture Content on the Tar Characteristic of Wood Pellet Feedstock in a Downdraft Gasifier. *Appl. Sci.* **2020**, *10*, 2760. [CrossRef]
19. Jenkins, S. Introduction to Pyrolysis and Gasification. In Proceedings of the Saskatchewan Waste Reduction Council Waste-to-Energy Workshop, Saskatoon, SK, Canada, 14–16 July 2020.
20. Ewald, A.; Spliethoff, H.; Fendt, S. Entrained Flow Gasification of Sewage Sludge–Performance Parameters and the Fate of Phosphorus, Potassium, Sulfur, and Heavy Metals. *Energy Fuels* **2025**, *39*, 2616–2629. [CrossRef]
21. Ram, M.; Mondal, M.K. Biomass gasification: A step toward cleaner fuel and chemicals. In *Biofuels and Bioenergy*; Gurunathan, B., Sahadevan, R., Zakaria, Z.A., Eds.; Elsevier: Amsterdam, The Netherlands, 2022; Chapter 13; pp. 253–276.
22. Sebastiani, A.; Parrillo, F.; Ardolino, F.; Arena, U.; Iannello, S.; Materazzi, M. Modelling of oxygen-steam gasification of waste feedstock in industrial fluidized bed reactors. *Chem. Eng. J.* **2025**, *506*, 159763. [CrossRef]
23. Gao, Y.; Wang, M.; Raheem, A.; Wang, F.; Wei, J.; Xu, D.; Song, X.; Bao, W.; Huang, A.; Zhang, S.; et al. Syngas Production from Biomass Gasification: Influences of Feedstock Properties, Reactor Type, and Reaction Parameters. *ACS Omega* **2023**, *8*, 31620–31631. [CrossRef] [PubMed]
24. Bonilla, J.; Gordillo, G.; Cantor, C. Experimental Gasification of Coffee Husk Using Pure Oxygen-Steam Blends. *Front. Energy Res.* **2019**, *7*, 127. [CrossRef]
25. AlNouss, A.; McKay, G.; Al-Ansari, T. A comparison of steam and oxygen fed biomass gasification through a techno-economic-environmental study. *Energy Convers. Manag.* **2020**, *208*, 253–276. [CrossRef]
26. Mavukwana, A.; Jalama, K.; Harding, K. Simulation of South African corncob gasification with Aspen Plus: A sensitivity analysis. *Appl. Mech. Mater* **2014**, *492*, 386–391. [CrossRef]
27. Susastriawan, A.A.P.; Saptoadi, H.; Purnomo. Small-scale downdraft gasifiers for biomass gasification: A review. *Renew. Sustain. Energy Rev.* **2017**, *76*, 989–1003. [CrossRef]
28. Cvetinović, D.; Erić, A.; Milutinović, N.; Petrov, N.; Andelković, J.; Bakić, V. Thermodynamic equilibrium modeling of biomass gasification: Effects of operating conditions on gasifier performance. *J. King Saud Univ.-Sci.* **2024**, *36*, 103370. [CrossRef]
29. Yabandeh, S.; Hajinezhad, A.; Moosavian, S.F.; Fattahi, R. Modeling and simulation of waste tire-based power generation system using Aspen Plus. *Results Eng.* **2025**, *28*, 107326. [CrossRef]
30. Aentung, T.; Thongchawee, A.; Wu, W.; Patcharavorachot, Y. Modeling of Liquid Fuel Production from Water Hyacinths and Waste Tires: A Comparative Study of Direct and Indirect Methods. *Preprints* **2024**, 2024011350.
31. Zhou, S.; Zhao, Q.; Yu, T.; Yao, X. Co-pyrolysis of Sewage Sludge with Paint Sludge: Kinetics and Thermodynamic Analysis via Iso-conversional Methods. *J. Wuhan Univ. Technol.-Mat. Sci. Edit.* **2024**, *39*, 716–727. [CrossRef]
32. Papuga, S.; Djurdjevic, M.; Tomovic, G.; Ciprioti, S.V. Pyrolysis of Tyre Waste in a Fixed-Bed Reactor. *Symmetry* **2023**, *15*, 2146. [CrossRef]
33. Li, W.; Wang, C.; Song, Y. Simulation of waste tire gasification in bubbling fluidized bed by Aspen: Contribution ratio analysis. *Renew. Energy* **2024**, *222*, 119995. [CrossRef]
34. Paiva, M.; Vieira, M.; Gomes, H.T.; Brito, P. Simulation of a Downdraft Gasifier for Production of Syngas from Different Biomass Feedstocks. *ChemEngineering* **2021**, *5*, 20. [CrossRef]
35. Ajorloo, M.; Ghodrat, M.; Scott, J.; Strezov, V. Recent advances in thermodynamic analysis of biomass gasification: A review on numerical modelling and simulation. *J. Energy Inst.* **2022**, *102*, 395–419. [CrossRef]
36. Tewari, K.; Balyan, S.; Jiang, C.; Robinson, B.; Bhattacharyya, D.; Hu, J. Unlocking Syngas Synthesis from the Catalytic Gasification of Lignocellulose Pinewood: Catalytic and Pressure Insights. *ACS Sustain. Chem. Eng.* **2024**, *12*, 4718–4730. [CrossRef] [PubMed]
37. Spiewak, K.; Czerski, G.; Bijak, K. The Effect of Temperature-Pressure Conditions on the RDF Gasification in the Atmosphere of Steam and Carbon Dioxide. *Energies* **2021**, *14*, 7502. [CrossRef]
38. Milioni, A. Gasification Process. Chemical Engineer—On Contract Cooperator—University UCBM—Rome (Italy). n.d. Available online: https://www.oil-gasportal.com/gasification-process/?print=print (accessed on 19 September 2025).
39. DOE NETL. 2023. Available online: https://netl.doe.gov/research/coal/energy-systems/gasification/gasifipedia/cleanup (accessed on 11 October 2025).

40. Brandstätter, G.; Fürsatz, K.; Long, A.; Hanni, T.; Schubert, T. Exploring the potential of sewage sludge for gasification and resource recovery: A review. *Environ. Technol. Innov.* **2025**, *40*, 104346. [CrossRef]
41. Yu, X.; Yu, D.; Yu, C.; Cai, M.; Han, J.; Liu, Y.; Liu, F.; Xu, M. Mineral evolution and catalytic mechanism in catalytic gasification of petroleum coke with coal/biomass ash. *Fuel* **2024**, *360*, 130582. [CrossRef]
42. Serrano, D.; Horvat, A.; Batuecas, E.; Abelha, P. Waste tyres valorisation through gasification in a bubbling fluidised bed: An exhaustive gas composition analysis. *Renew. Energy* **2020**, *200*, 1438–1446. [CrossRef]
43. Gil-Lalaguna, N.; Sánchez, J.L.; Murillo, M.B.; Rodríguez, E.; Gea, G. Air–steam gasification of sewage sludge in a fluidized bed. Influence of some operating conditions. *Chem. Eng. J.* **2014**, *248*, 373–382. [CrossRef]
44. Schweitzer, D.; Gredinger, A.; Schmid, M.; Waizmann, G.; Beirow, M.; Spörl, R.; Scheffknecht, G. Steam gasification of wood pellets, sewage sludge and manure: Gasification performance and concentration of impurities. *Biomass Bioenergy* **2018**, *111*, 308–319. [CrossRef]
45. Simanjuntak, J.P.; Zainal, Z.A. Experimental study and characterization of a two-compartment cylindrical internally circulating fluidized bed gasifier. *Biomass Bioenergy* **2015**, *77*, 147–154. [CrossRef]
46. Thomson, R.; Kwong, P.; Ahmad, E.; Nigam, K.D.P. Clean syngas from small commercial biomass gasifiers; a review of gasifier development, recent advances and performance evaluation. *Int. J. Hydrogen Energy* **2020**, *45*, 21087–21111. [CrossRef]
47. Cortazar, M.; Santamaria, L.; Lopez, G.; Alvarez, J.; Zhang, L.; Wang, R.; Bi, X.; Olazar, M. A comprehensive review of primary strategies for tar removal in biomass gasification. *Energy Convers. Manag.* **2023**, *276*, 116496. [CrossRef]
48. Wang, L.; Zhou, T.; Hou, B.; Yang, H.; Hu, N.; Zhang, M.A. Comprehensive Review of Biomass Gasification Characteristics in Fluidized Bed Reactors: Progress, Challenges, and Future Directions. *Fluids* **2025**, *10*, 147. [CrossRef]
49. Niu, M.; Xie, J.; Liang, S.; Liu, L.; Wang, L.; Peng, Y. Simulation of a new biomass integrated gasification combined cycle (BIGCC) power generation system using Aspen Plus: Performance analysis and energetic assessment. *Int. J. Hydrogen Energy* **2021**, *46*, 22356–22367. [CrossRef]
50. Ramalingam, S.; Rajendiran, B.; Subramiyan, S. Recent advances in the performance of Co-Current gasification technology: A review. *Int. J. Hydrogen Energy* **2020**, *45*, 230–262. [CrossRef]
51. Acevedo-Páez, J.C.; Durran, J.M.; Posso, F.; Arenas, E. Hydrogen Production from Palm Kernel Shell: Kinetic Modeling and Simulation. *Int. J. Hydrogen Energy* **2020**, *45*, 25689–25697. [CrossRef]
52. Khezri, S.M.; Shariat, S.M.; Tabibian, S. Reduction of pollutants in painting operation and suggestion of an optimal technique for extracting titanium dioxide from paint sludge in car manufacturing industries—Case study (SAIPA). *Toxicol. Ind. Health* **2011**, *28*, 463–469. [CrossRef]
53. Le-Phuc, N.; Pham, Y.T.H.; Bui, P.N.V.; Luong, T.N.; Vo, P.N.X.; Ngo, P.T.; van Tran, T.; Nguyen, D.A.; Wenzel, M.; Gloe, K.; et al. Towards efficient extraction of La(III) from spent FCC catalysts by alkaline pre-treatment. *Miner. Eng.* **2018**, *127*, 1–5. [CrossRef]
54. Yang, Z.; Hu, Q.; Chen, Q.; Chen, Y.; Li, H.; Yang, H.; Chen, H. Numerical study on the steam gasification of biomass in a 100 kW dual fluidized bed gasifier. *Energy Fuels* **2024**, *38*, 4273–4289. [CrossRef]

Disclaimer/Publisher's Note: The statements, opinions and data contained in all publications are solely those of the individual author(s) and contributor(s) and not of MDPI and/or the editor(s). MDPI and/or the editor(s) disclaim responsibility for any injury to people or property resulting from any ideas, methods, instructions or products referred to in the content.